

Enhanced Deep Learning Framework for the Detection of Crop Leaf Diseases

Manju Bagga*, Sonali Goyal

Maharishi Markandeshwar Engineering College, MMICT&BM, Computer science and Engineering Department, Maharishi Markandeshwar (Deemed to be University), Mullana, Ambala, Haryana, India.

*Corresponding Author's Email: rathi.ancestor@gmail.com

Abstract

Crop diseases significantly impact food production, making their early identification crucial for farmers. In India alone, over 43,000 acres are dedicated to stone fruit cultivation, producing approximately 0.25 million tons annually. Identifying diseases in fruit leaves with the naked eye poses challenges due to the complexity of damaged leaf images, which often exhibit irregular shapes, varying sizes, rich colors, blurry boundaries, and cluttered backgrounds. Effective disease management relies on precise segmentation of plant leaf images, a task that has become more feasible with advancements in deep learning and graphics processing unit (GPU) technology. This study proposes an enhanced ResU-Net model aimed at improving the performance of deep convolutional neural networks while reducing the number of parameters. The model incorporates ResNet50's skip connections in the encoder, enhancing the transfer of feature information between the contraction and expansion paths of the U-Net architecture. This customization improves the model's capability in segmenting diseased plant leaves. By combining convolutional blocks in the decoder with encoder skip connections, the model achieves superior expression ability. The proposed ResU-Net model demonstrated robust performance, achieving training, validation, and testing accuracies of 94.07%, 94.21%, and 95.00%, respectively. When compared to other existing methods, the results validate the model's effectiveness in addressing the plant leaf segmentation problem. This approach offers a promising solution for efficient and accurate identification of crop diseases, contributing to improved agricultural practices.

Keywords: Convolutional Neural Networks, Deep Learning, Resnet50, Segmentation, Stone Fruits Leaf Diseases, U-Net.

Introduction

Agriculture and concomitant areas are the main roots of income for most of the nations. The preservation and security of agricultural supply are among a country's most fundamental and important needs. In developing nations like India, malnutrition is a persistent issue that is directly related to nutritional sufficiency. Farming practices within a nation are based on the quantity and quality of its commodities, particularly crops. Diseases affecting leaf tissue, stems etc. have a major impact on agricultural productivity, negatively affecting the progress of harvests and resulting in losses to the environment, society, as well as economy (1). The following stone fruits are planted on over 43,000 acres in India alone, and they yield about 0.25 million tons of fruit annually: mango, peach, apricots, olives, nectarines, plums, and cherries (2). If fruit wines are produced, then orchardists can profitably increase their fruit supply, which will create jobs and increase their

profits. Stone fruit infections can be triggered by a wide diversity of factors, including as biotic components, atmospheric pressure, environment, and nutriment. Stone fruits' leaves are particularly susceptible to diseases throughout the growing season (such as ring, rust, early leaf disease, scab, gall midge etc.). Leaf diseases can also easily alter the colour of the leaves, and in severe situations, they can even cause the leaves to fall off the tree and weaken the fruit tree's resistance to disease, which lowers the quantity or quality of fruit produced (3). Thus, treating and preventing leaf diseases is crucial for the development of stone fruits. Detecting disease symptoms on leaves by hand proves to be a challenging in large orchards but attainable task for very small farms. Even the most skilled agronomist and plant pathologists struggle to identify particular diseases, either one-off or multi-off. Consequently, incorrect conclusions and interpretations were drawn.

This is an Open Access article distributed under the terms of the Creative Commons Attribution CC BY license (<http://creativecommons.org/licenses/by/4.0/>), which permits unrestricted reuse, distribution, and reproduction in any medium, provided the original work is properly cited.

(Received 13th January 2025; Accepted 22nd April 2025; Published 30th April 2025)

Using plant characteristics to detect physical appearances in response to organic matters (biotic) and temperature (abiotic) components including low water, low light, bacteria, fungi, and other factors is crucial for plant and agricultural development. Nutrient-starved plants will eventually turn sick. There are two types of nutrients that plants need: macronutrients and micronutrients. Among other nutrients, macronutrients include nitrogen, calcium, potassium, sulphur, phosphorus, and magnesium. Micronutrients including iron, copper, zinc, and chlorine are only necessary in trace amounts for plants. By measuring the height of the plant, counting the leaves, and assessing the thickness of the leaves, the shortages in nitrogen, phosphorus, potassium, and calcium were identified. It will therefore impact the fruit's quality and productivity. Depending on the source, a plant may get an infection from a range of lesions in a different way. Pests and diseases that kill trees and result in losses and reduced yield are some of the major challenges faced by growers of stone fruits as well as other crops. The decision of whether or not chemicals are needed for production is typically made by experts. Crop treated with more and more chemicals are extremely unhealthy. In recent years, crop security methods have grown increasingly automated. Examples of these technologies include smart android phones and expert system like machine learning and deep learning applications for disease categorisation (4). Consequently, several investigators have resorted to image enhancement methods to help agronomists accomplish this challenging task. Currently, identification of diseases on plant leaves uses expert map querying and automated picture processing. Manually identifying lesions using the old method is exorbitant, prolonged, and untrustworthy. Despite the fact that technology currently makes it practicable to identify related issues that significantly affect the growth of the leaves on stone fruits (5). The fastest identification speed, poor accuracy, and adverse environmental effects of the most recent computer-aided recognition technique have prevented it from being widely used. Therefore, in order to improve the model's capacity for generalisation, it is essential to construct a stone fruit leaf disease identification system that can make prompt and errorless decisions regarding plant leaf infections

by blending datasets that represent a broad spectrum of crops and locations (6). Because most of the researchers worked on single datasets rather than hybrid datasets. Models trained on single dataset for particular crop may not work efficiently on another dataset of same crop. Among the various approaches, Deep Learning (DL) methods that use convolutional neural network and are based on artificial intelligence performed well in image identification tests. One artificial neural network that is frequently used for picture identification is convolutional neural network (CNN) (7). In the field, automatic detection and picture categorisation present certain difficulties. The complexity of the background, which complements the lesion's subject, unnecessary noise, lighting variations, equipment, camera angle, and extras like unwanted grass, soil, roots, and overlapping of leaves are all factors are considered (8). It is imperative to recognise and separate these elements. One technique for separating polluted areas from the collected images is segmentation. The suggested automatic method must remove unnecessary elements from the image and isolate only the desired portion in order to efficiently identify diseases in the fields and enable real-time plant disease identification. Identifying lesions rather than merely categorising them is of main concern (9). The categorisation by itself will not yield adequate results until it is combined with the disease's position. Using both segmented and non-segmented photographs, the accuracy of plant leaves was investigated (10). Using segmented images, the network reached an accuracy of 98.6%, compared to just 42.3% with non-segmented images. The testing images were created using images that were sourced from the internet. The precision of evaluating crop disease severity and identifying crop illnesses is directly influenced by the segmentation of disease lesions in plant leaf images. Experimentation is focused on finding the most effective and high-quality ways to section damaged leaves from crops. Over the past twenty years, lesions have been extracted and identified using conventional imaging techniques such edge detection, thresholding, colour space conversion, watershed segmentation, feature transformation etc.

It has proven difficult to develop an automated system for detecting leaf disease in stone fruits (11). Many diseases can have symptoms that are

physically similar to one another, making it challenging to distinguish between them with more nuanced signs. Recent developments in computer vision have made it possible to reliably diagnose tomato flaws (12). This study looks at the different kinds of biotic leaf diseases that have been identified and categorised at an early stage through the use of deep learning technologies. The literature has been reviewed, and then the issue of segmentation and categorisation has been discussed. As the segmentation portion receives less attention. Not just a diseased area, but a fully clear area is the focus of attention. Additionally, a more universal leaf segmentation technique that works in both controlled and uncontrolled settings needs to be created and put into practice. Pre-trained DL models have been used by numerous authors to investigate the categorisation of biotic leaf diseases. Once the dataset was pre-processed as part of the preliminary stage of image processing, researchers used feature classification techniques to identify the disease's patches. Up until now, the classification model has not been able to reliably identify the boundaries of the lesion. To achieve greater accuracy from a variety of datasets, this work has suggested the robust hybrid Residual U-Net (HRU) model, that partitions the lesion items following pre-formatting of unstructured raw data. To achieve semantic segmentation and localisation of spots or blotches within leaf image, we employ the U-Net convolutional network symmetric architecture i.e. most popularly used as semantic segmentation model with a residual network as ResNet-50 as backbone (13, 14).

The core contributions of our proposed hybrid Residual U-Net (HRU) model are as follows: To down-sample the input features of stone fruit leaf lesions, an HRU model is presented, with ResNet-50 serving as the encoder part of the U-Net model. To derive high-level feature maps of the infected area, down-sampling is performed. The properties of lesion areas are contained in these high-level feature maps; they are combined with the high-level feature maps from the encoder portion after being up-sampled in the U-Net decoder part. As our study is built on pixel-wise observations employing full deep learning segmentation networks, it has better expandability and general applicability. Lastly, we discussed our model's

performance evaluation and contrasted it with other findings that had been published.

Building upon these motivations, it is essential to examine recent advancements in semantic segmentation and its application to crop disease detection. Semantic segmentation is a task that has garnered a lot of attention lately, not only from the computer vision community but also from other fields where automated image annotation is a crucial process, such as crop disease detection, remote sensing, medical imaging, grocery detection, etc. Specifically, specialised methods have been developed across several fields because the computer vision community does not need to handle certain task-specific characteristics (and vice versa). Plant disease detection has shown deep learning to be an effective approach (15). In comparison to machine learning, researchers can get far higher recognition accuracy by simply designing the network architecture and adjusting the hyper parameters (16). Researchers proposed a segmentation technique to determine the disease severity (17). Furthermore, a modified rectified linear unit (ReLU) has been developed, which compared and merged the earlier research approaches and performed exceptionally well, with an average accuracy of 93.4%. Nevertheless, the amount of model parameters is excessive, and this segmentation approach significantly decreased the accuracy of image detection with complicated backgrounds (18).

After pre-processing and feature extraction, the whale optimisation algorithm is applied for feature selection (19). An optimised artificial neural network was utilised for the study of olive leaves. The data is classified by the artificial neural network using multilayer perceptron technique, which improves prediction accuracy. When contrasting with current models, the suggested model performs much better in F1-score, Accuracy, Precision, and Recall. The innovative model achieves an accuracy of approximately 96.00% for categorization tasks and 97.00% for classifying objects into two distinct classes. A study used red green blue (RGB) and multi-spectral photos taken in a controlled setting to assess a dataset of both healthy and defective plant components. It was studied how each spectral channel and various camera kinds affected the ability to identify diseases. After segmenting and detecting leaves using Fast R-CNN and Mask R-

CNN, leaves were classified using the Inception Version3 network to distinguish between healthy and diseased leaves. The assessment of disease levels in olive trees in the field was made possible by the combination of these instruments (20). Several deep neural network prototypes for disease recognition were taken into consideration in order to aid in the early detection of disease. This paper outlines many fungal plants diseases emerged as blotches on the surface of leaf and the processes that lead to host changes and environmental variation in them. Failure to recognize and distinguish fungal leaf diseases at an early stage can result in a significant loss of crop output (21). The author proposed a multi-level deep learning prototype for both early and late blight disease detection and classification. The first stage of the prototype used an image segmentation technique leveraging YOLO version 5, while the second stage used a novel deep learning system based on convolutional neural network (22). The planned prototype was tested on a dataset with 4,062 photos, and it achieved 99.7% accuracy. After adjusting the contrast and brightness of the image, the author used bipolar thresholding and further segmentation techniques (23). To identify rice crops that are unhealthy, they employ a combination of photo processing techniques and soft computing. When implemented correctly, the technique's basic principle was sound. With a median recognition correctness of only 82% across the four datasets, it is evident that further work is required. In a recent study, scientists combined feed-forward neural networks with a hybrid meta-heuristic feature selection strategy to propose an early disease classification method for mango leaves. Their technique, which made use of artificial neural networks, produced a high accuracy of 89.41%. The results of this study could greatly enhance the early identification and categorisation of illnesses in mango trees, hence lowering crop losses and raising agricultural output (24). ResNet frequently acts as the foundation for feature extraction in the detection of objects and pixel-level (semantic) segmentation; when paired with other architectures (such as Faster region-based CNN, Mask region-based CNN, and U-Net), it can offer powerful feature (edge, shape etc.) depiction capabilities (25). The asymptotic non-local mean image algorithm was

the foundation for the peach disease detection technique presented by the authors in order to overcome problems with like visual clutters in image (noise), background distortion, and suboptimal detection performance in diseased images of peach. Their tests demonstrated the efficacy of this strategy for peach disease identification (26).

The following sections comprise the remaining paper: The next section i.e. Section 2 is crucial as it specifies the materials and segmentation technique utilised in this work; Section 3 discusses the various performance evaluation metrics; Section 4 discusses the hybrid model's comparison with other models and with other published results; and Section 5 analyzes the conclusion section.

Methodology

An outline of the leaf image dataset and methodology for identifying illnesses in stone fruit leaves is provided in this section. We will first go over the dataset that we used for our study, and then we will quickly go over the image pre-processing step. We shall talk about the history of the current ResNet-50 and U-Net architectures later.

Leaf Image Dataset

The mangos, olive, and peach leaf samples that are utilised to assess the performance are taken from a variety of datasets. MangoLeafBD, CNN_Olive, and Plant Village datasets are available for mango, peach, and olive, respectively. To balance the dataset, some photos were also gathered from the internet. Of the three stone fruits, there are a total of nine classes—two unhealthy and one healthy. Every crop has 700 photos in its healthy class. Diseased classes, as shown in Table 1, also include 700 photographs each, with the exception of peach rust, which has 500 images. There are actually 6100 photos in total, images of biotic stress infected by bacteria and fungi are included in the dataset. Six types of augmentation are applied as mentioned in data pre-processing section, so 6100*6 becomes 36,600 images. After then, an 8:1:1 ratio was used to partition the whole dataset into sets of training, validation, and testing. Sample images of several types of leaf diseases in stone fruits are displayed in Figure 1.

Table 1: Data Description of Diseases of Stone Fruits Leaves

Stone Fruit Name	Disease Category	Disease Scientific Name	Type of Disease	Total Images
Mango	Powdery Mildew	<i>Oidium mangiferae</i>	Fungal	700
	Mango Gall Midge	<i>Procontarinia mattei</i>	Bacterial	700
Olive	Aculus Olearius	<i>Aceria oleae</i>	Fungal	700
	Peacock Spot	<i>Spilocaea oleaginea</i>	Fungal	700
Peach	Bacterial Spot	<i>Xanthomonas arboricola</i>	Bacterial	700
	Peach Rust	<i>Tranzchelia discolor</i>	Fungal	500

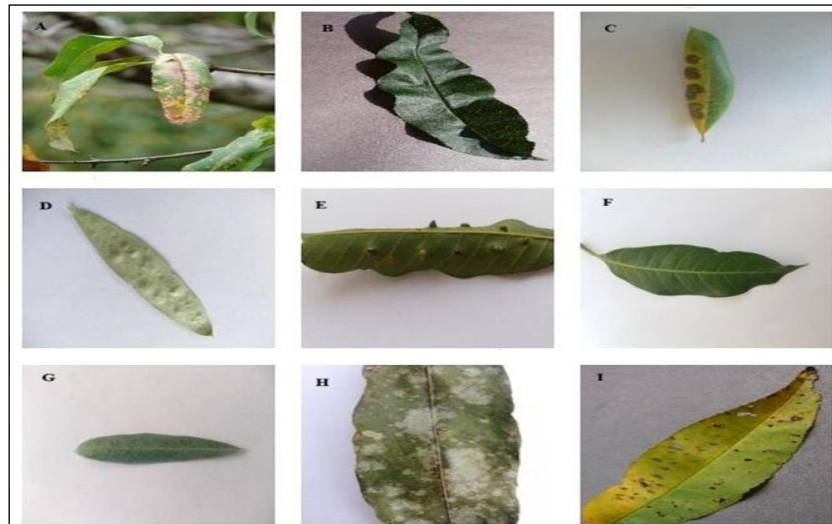


Figure 1: Sample Images of Stone Fruits A) Peach Rust B) Peach Healthy C) Olive Peacock D) Olive Aculus E) Mango Gall Midge F) Mango Healthy G) Olive Healthy H) Mango Powdery Mildew I) Peach Bacterial Spot

Data Pre-Processing

A crucial step in image processing and computer vision is picture pre-processing. It is a technique for manipulating images to produce improved images or to extract pertinent data from them because machine or deep learning model requires processed input, its performance degrades on raw data. Learning of raw data is not advanced yet so it consists of basic operations like scaling, contrast enhancement, noise reduction, sharpening and smoothing images, and sophisticated procedures like segmenting images (27). Image processing is the process of manipulating photographs to extract information, highlight or de-emphasise certain information, or analyse images to uncover information that is concealed. A picture's processing includes making it look better and accurately represent the input image so that it may be used for the intended purpose. Pre-processing reduces artefacts, which enhances the quality of the data. Farmers might gain a lot from this technology by being able to spot diseases early,

which would allow for prompt action and better crop management. The pre-processing procedures for images come in several varieties and are explained below. To increase the generalizability of the model and prevent over fitting, six types of data augmentation techniques were applied during training. These include: rotation, which randomly alters the orientation of leaves; brightness variation, to simulate lighting changes and improve model adaptability; shearing, which introduces perspective distortions; zoom, which allows the model to learn features at different scales; and horizontal and vertical flips, which help the model recognize leaf structures regardless of direction. These augmentations effectively expanded the training set by creating diverse variations of the original data, enabling the model to become more robust against real-world distortions. As a result, the model demonstrated improved accuracy and lesion localization during testing, even in images with challenging backgrounds and orientations.

The Methodological Foundation of the RseNet-50 and U-Net Architectures

This section covers the current architectures of ResNet-50 and U-Net.

U-Net Architecture: The U-Net model, which is employed in the majority of recent literature, is examined in this section. Convolutional neural networks are used in U-Net architecture to efficiently capture context-based data and provide precise localisation. The encoder and the decoder are the two fundamental parts of the U-Net design (28). The first and second portions of the model are created by these components, respectively. The encoder, which is often referred to as the contraction path, takes features out of the input image. As a backbone, it uses CNN architectures that have already been trained, including ResNet, VGG, Inception, or Dense-Net. The encoder of the U-Net design uses two successive blocks of unpadded 3 x 3 convolutions. After that, there is an activation function ReLU (Rectified Linear Unit) with a 2 x 2 carpooling and a down sampling stride of 2. At each stage of the down sampling process, the number of features is increased by twice, supporting the input image's encoding at various levels into feature map representations. Conversely, the second component of the U-Net architecture is the decoder, which is also referred to as the expanded path. In order to achieve higher

resolution, it attempts to recreate the segmentation by extruding the differential features that the encoder trained into the pixel grid. Every stage of the decoder entails up sampling the feature map and then performing a 2 x 2 up-convolution, which diminish the feature channels by 50%. Furthermore, the up-sampled feature map is concatenated with the feature or activation maps cut from the relevant place in the contracting route. ReLU activation follows each of the two consecutive 3 x 3 convolutions that have been applied. There are 23 convolutional layers in the U-Net model. The U-Net model, which was first presented in 2014, makes use of the idea of classification per pixel in order to separate biological images semantically. It is frequently used in imaging to pinpoint particular areas of an image, usually those with abnormalities. Semantic segmentation allows for accurate localisation of items or areas of interest since, in contrast to classification, the input and output have their original shape. Figure 2 displays the U-Net architecture. The final layer in the architecture is a 1 x 1 convolutional layer, which maps a feature array with 64 elements to a predetermined number of class categories. The ResNet design, which serves as the network's backbone, took the place of the U-Net model's encoder layers in our suggested method.

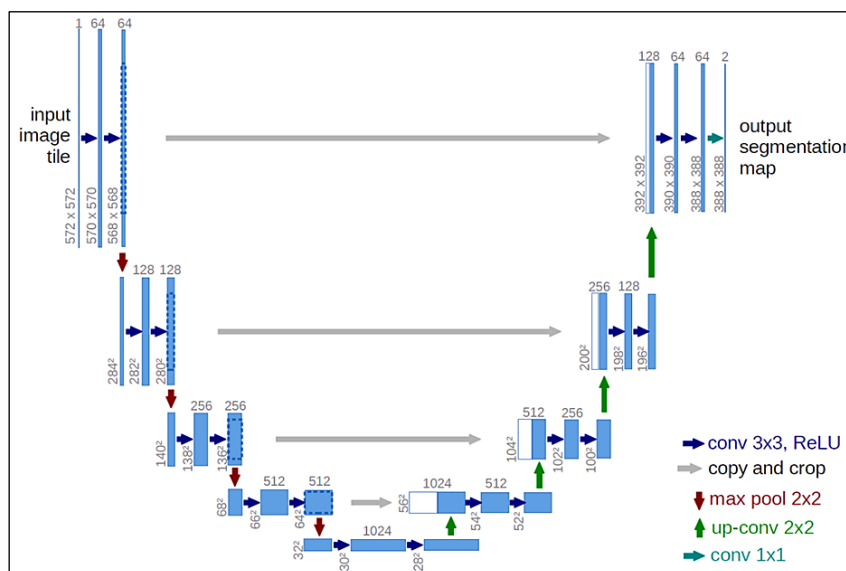


Figure 2: Overall U-Net Architecture for Image Semantic Segmentation (28)

Res-Net Architecture: To solve the problem of degrading or disappearing gradient that arises in deep convolutional neural networks, Res-Net was

introduced (14). Deeper networks typically deteriorate as they converge; this isn't because of high variance or over fitting, instead of a drop in

training performance. This degrading issue is effectively resolved by the Res-Net architecture, which directly maps the stacked layers to residual mapping. Res-Net explicates further a mapping termed $J(x) = K(x) - x$, where $K(x)$ reflects the intended fundamental mapping, as opposed to previous systems where the intended underlying mapping was explicitly translated to the layers on top. This residual mapping is then mapped to the

stacked no-linear layers. One way to express the original mapping is as $J(x) + x$. The main conjecture is that residual mapping optimisation is less complicated than unreferenced mapping optimisation. "Shortcut connections" are used in the feed forward network to implement the $J(x) + x$ formulation. Figure 3 provides the fundamental building component of residual learning.

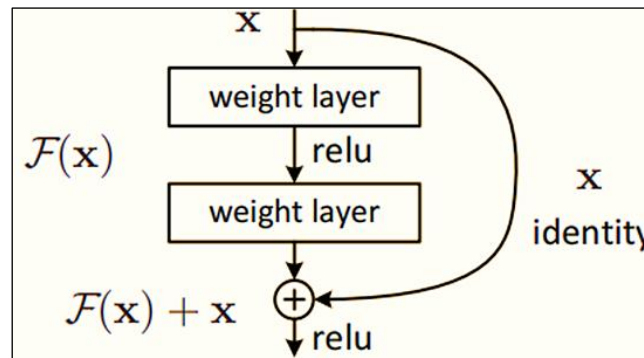


Figure 3: Fundamental Component of Residual Learning

"Identity mappings" are made possible by Res-Net's shortcut connections, which combine the outputs of these connections with the outputs of the stacked top layers. Crucially, there is no additional processing overhead associated with these identity mappings. In contrast to conventional models, which lose accuracy as depth

increases, deep residual networks—like Res-Net—show enhanced accuracy as depth increases. For the purpose of semantic segmentation in our suggested model, we leverage the ResNet50 architecture as the foundation of the U-Net model. Figure 4 represents the convolutional layers of ResNet50 for a range of parameters.

Layer Name	Output Size	50-Layer Resnet
Conv1	112 x 112	$7 \times 7, 64, \text{stride } 2$
Conv2_x	56×56	$3 \times 3 \text{ max pool, stride } 2$
Conv3_x	28×28	$\begin{pmatrix} 1 \times 1, 64 \\ 3 \times 3, 64 \\ 1 \times 1, 256 \end{pmatrix} \times 3$
		$\begin{pmatrix} 1 \times 1, 128 \\ 3 \times 3, 128 \\ 1 \times 1, 512 \end{pmatrix} \times 4$
Conv4_x	14×14	$\begin{pmatrix} 1 \times 1, 256 \\ 3 \times 3, 256 \\ 1 \times 1, 1024 \end{pmatrix} \times 6$
Conv5_x	7×7	$\begin{pmatrix} 1 \times 1, 512 \\ 3 \times 3, 512 \\ 1 \times 1, 2048 \end{pmatrix} \times 3$
FLOPs	1×1	average pool, 1000-d fc, softmax 3.8×10^9

Figure 4: 50-Layer Architecture of ResNet

Proposed Methodology

This section contains a detailed description of our proposed hybrid model, called the hybrid Residual U-Net (HRU) model. It is based on two deep convolutional neural networks: one called

ResNet50, which is specifically designed for image classification, and another called U-Net, which is specifically designed for image segmentation. Instead of treating the entire leaf, this hybrid model is specially developed to work on the

afflicted area of the leaf. We have provided an overview of our suggested HRU model in this section. Because there are comparable or overlapping afflicted regions inside lesion sites, segmenting them is a highly difficult task. We have developed a unique semantic segmentation technique for stone fruit leaf lesions in order to address this difficulty. Figure 5 depicts the proposed model's overview. Like the original U-Net, the suggested model consists of two major components: Up-sampling path: an encoder and

down-sampling path: a decoder (28). ResNet-50 architecture takes the place of the encoder component (14). The foundation of the U-Net architecture is the ResNet-50. To improve and increase its effectiveness in leaf disease detection, the original ResNet-50 architecture has undergone a number of changes. The input picture of the infected leaf is down-sampled by the ResNet-50 encoder component. The decoder portion then up-samples the pixels.

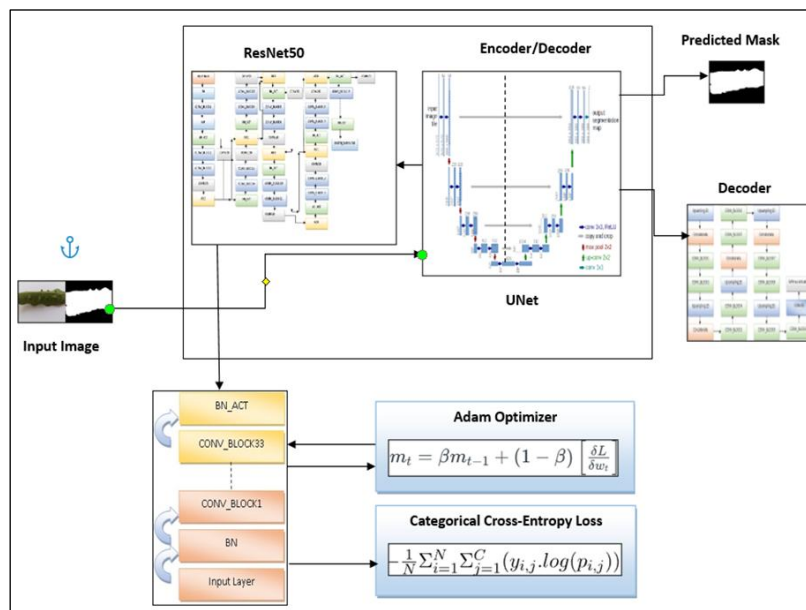


Figure 5: Basic Layout of Proposed HRU Model

To take advantage of the residual mapping, we have swapped out the U-Net encoder block with the Res-Net design in the suggested work. Figure 6 depicts the network's proposed architecture. This represents the batch normalisation (BN), maxpooling (MP), and batch normalisation and ReLU activation function (BN_ACT), which are utilised in all of the model's intermediate layers. Furthermore, as seen in Figure 7, the CONVIONAL_BLOCK i.e. conv_block stands for the activation layer, batch normalisation, and convolution layer. Figure 6 depicts half of the architecture; the two arrows therein denote the zero-padding layer. There are 33 CONVIONAL_BLOCKS i.e. conv_blocks in total, however only 16 are shown here because of space restrictions. The remaining CONV_BLOCKS have the same structure. Through zero padding, the two CONVIONAL_BLOCKS are connected. Figure 6 illustrates the addition portion that occurs after every two CONVIONAL_BLOCKS. This addition

section involves adding the previous addition layer to the current layer. Additionally, two 2D convolutional layer i.e. CONV2D layers are occasionally located after the activation layer. A part of the up-sampling layers are concatenated by means of these activation functional layers. There is a final batch normalisation layer and activation function layer after CONVIONAL_BLOCK 33. The section on up-sampling then begins. Figure 8 depicts the up-sampling block's whole construction. There are two CONVIONAL_BLOCKS and a concatenate layer once the layer has been up-sampled. The non-linear functions from the decoder i.e. activation function portion to the up-sampling layer of the decoder are concatenated by all four concatenation layers. In order to simplify the idea, let's break down the architecture. The U-Net model is made up of two paths down sampling path and up sampling path i.e. an encoder and a decoder. ResNet50 is employed in the encoder,

whereas upsampling is done in the decoder. The encoder can be shown as follows:

$$E(x) = ResNet50(x) \dots \dots \dots [1]$$

The decoder can be represented as:

$$D(z) = Upsample(z) \dots \dots \dots [2]$$

With 50 layers, Res-Net50 is a deep residual network that uses an encoder. One way to depict the leftover block is as follows:

$$y = F(x, \{W_i\}) + x \dots \dots \dots [3]$$

where the input is (x) and the residual function is (F(x, {W_i})).

Decoder (Upsampling): Upsampling is carried out via the U-Net's decoder component, and it is represented as:

$$Upsample(z) = ConvTranspose2D(z) \dots \dots \dots [4]$$

Where the encoded feature map is denoted by (z).

The following equations are used by the Adam optimiser to update the weights:

$$m_t = \alpha_1 m_{t-1} + (1 - \alpha_1) g_t \dots \dots \dots [5]$$

$$v_t = \alpha_2 v_{t-1} + (1 - \alpha_2) g_t^2 \dots \dots \dots [6]$$

$$\hat{m}_t = \frac{m_t}{1 - \alpha_1^t} \dots \dots \dots [7]$$

$$\hat{v}_t = \frac{v_t}{1 - \alpha_2^t} \dots \dots \dots [8]$$

$$\theta_{t+1} = \theta_t - \beta \frac{\hat{m}_t}{\sqrt{\hat{v}_t + \epsilon}} \dots \dots \dots [9]$$

where the gradient is g_t , the learning rate is β , the first and second moment estimates are m_t and v_t , the decay rates are α_1 and α_2 , and a tiny constant is ϵ . For multi-class classification, the categorical cross-entropy loss function is utilised, and it looks like this:

$$L = - \sum_{i=1}^N y_i \log(\hat{y}_i) \dots \dots \dots [10]$$

Where the projected probability for class (i) is represented by \hat{y}_i and the real label is denoted by y_i .

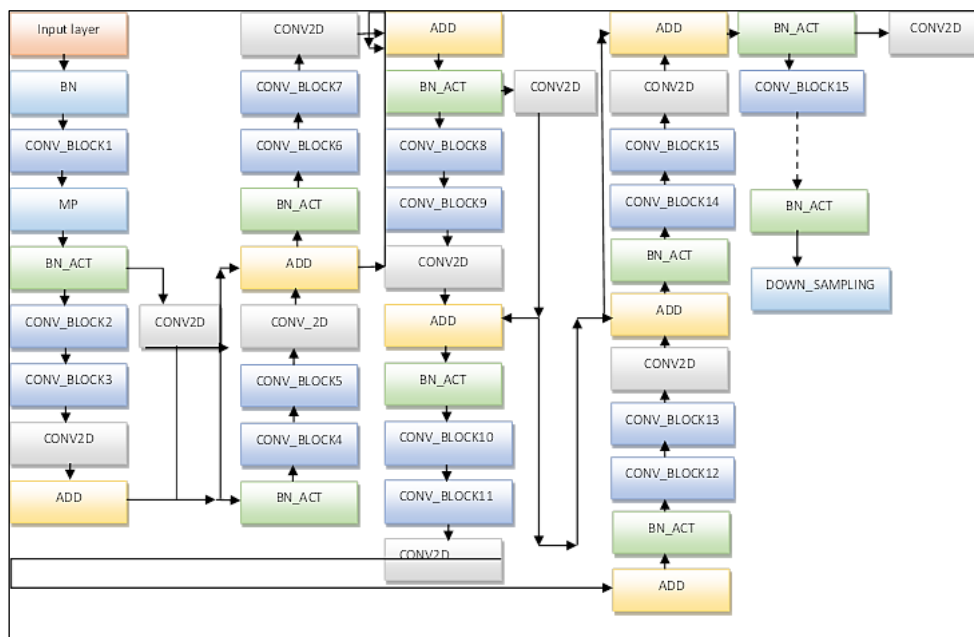


Figure 6: Architecture of ResNet50 as Encoder in Proposed HRU Model

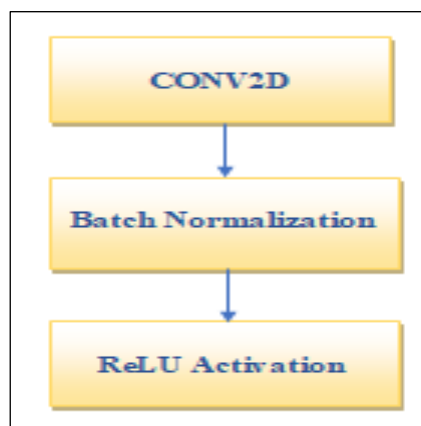


Figure 7: Convolutional block

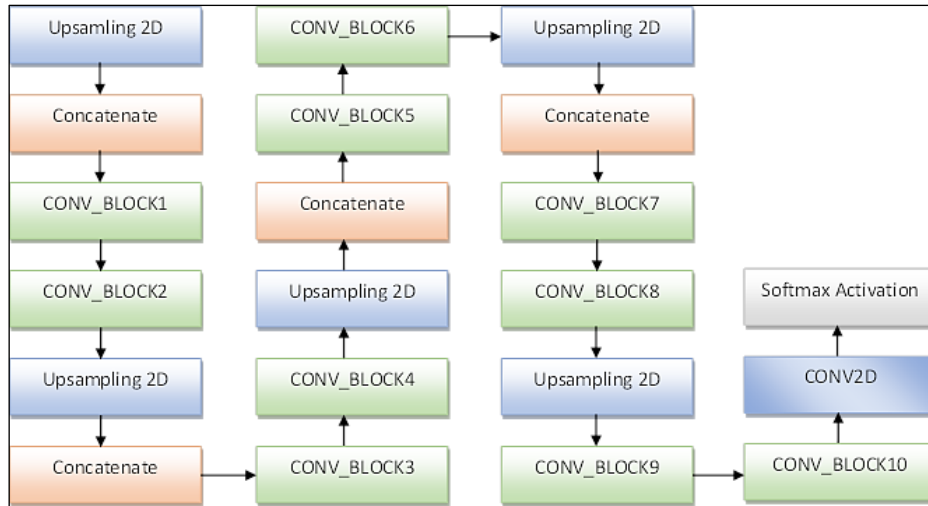


Figure 8: U-Net as Decoder in Proposed HRU Model

Performance Metrics

The HRU model's performance was assessed in this study utilising a number of parameters. Metrics including "Accuracy," "Precision," "Recall," "F1-Score," and "Mean Intersection over Union (mIoU)" were produced by computing the false positive:FP, false negative:FN, and true positive:TP. Among these, accuracy quantifies the percentage of cases that are accurately classified out of all the cases. Recall or in other terms also known as sensitivity, is the percentage of real positive cases in the total number of cases that actually fall into the positive category. Precision alternatively called positive predictive value, is the percentage of real positive instances in the total number of instances predicted to fall into the positive category. It is calculated as the ratio of TP:true positive and TN:true negative predictions to the total number of predictions (29). The F1-

score, which represents test accuracy, is the harmonic mean of recall and precision, with equally weighted factors. The mean intersection over union, or mIoU, is a commonly used metric to evaluate the segmentation performance of images (30). It quantifies the overlap that exists between the segmentation that is anticipated and the actual image. IoU is averaged to get mIoU. The following equations can be used to express the accuracy, precision, recall, F1-score, and mIoU: TP stands for true amount, which is the segmented diseased part that is correctly detected; FP stands for false positive, which is the stone fruit leaf disease that is incorrectly identified; FN stands for false negative, which is the stone fruit leaf diseased pixels that are present in the leaf's true truth area but are not recognised as such by an algorithm (shown below); TN represents the leaf disease's non-infected region as the actual diseased area.

$$Accuracy = \frac{TP + TN}{TP + TN + FP + FN} \dots\dots\dots [11]$$

$$Precision = \frac{TP}{TP + FP} \dots\dots\dots [12]$$

$$Recall = \frac{TP}{TP + FN} \dots\dots\dots [13]$$

$$F1 - Score = 2 * \frac{(Precision * Recall)}{Precision + Recall} \dots\dots\dots [14]$$

$$mIoU = \frac{1}{n} \sum_{i=1}^n IoU_i \dots\dots\dots [15]$$

Algorithm 1: HRU Model for Leaf Disease Detection in Stone Fruits**Input: Stone Fruit Dataset****Output: Region-of-Interest Segmented Image****Begin**

//Data Pre-processing

1. Collect labelled dataset of stone fruits leaf images containing healthy and diseased samples for mango, olive, and peach plants.
2. To guarantee interoperability with the network during training, resize photos to 256×256 resolution.
3. Augment the dataset to enhance model generalization.

//HRU model is proposed by concatenating ResNet50 and U-Net, Feature Extraction using ResNet50

4. To down-sample the input features of leaf lesions, load the pretrained ResNet50 as the backbone architecture in the encoder portion of the U-Net model. To extract the high-level feature maps of the lesion's area, down sampling is used.
5. The convolutional layers for stratified feature extraction were kept in place while certain layers were either added or removed from ResNet-50 as an encoder during the fine-tuning procedure.

//Combination with U-Net

6. Design U-Net for semantic segmentation and classification.
7. Connect the feature-extraction output from ResNet50 (Encoder) to the corresponding layers in the decoder part of U-Net.

//Training

8. Partition the dataset into training, validation and testing sets.
9. Fine-tune the integrated model on the training set, adjusting weights to adapt to the unique leaf characteristics of mango, olive, and peach plants.
10. The output is the image that was recognised from the input.
11. Validate the model on test dataset.

Results and Discussion

This section contains the results of the experiments we performed to evaluate the effectiveness of our suggested HRU model.

Experimental Setup

All experiments were conducted using Google Collaborator's GPU runtime (NVIDIA Tesla T4, NVIDIA-SMI 535.104.0) accessed from a Windows 11 PC with a 64-bit x64-based processor. The model was implemented using the Keras framework with Tensor Flow backend, which facilitated the training and validation of deep neural networks. The proposed hybrid Residual U-Net was trained and evaluated on hybrid datasets for segmenting diseased regions in stone fruit leaves. Next, a ratio of 80:10:10 was used to partition the whole dataset into training, validation, and testing sets. As the backbone model for the U-Net architecture, we used ResNet-50. The batch size that we used for our research was 32. We ran the suggested model for 25 epochs with

early stopping criteria in order to train it. A learning rate of 0.001 was used while using the ADAM optimiser. Table 2 has all of these parameter settings. Since the encoder weights from the Image Net dataset are the best learnt weights and perform exceptionally well, we utilised them to train our model. To maximise the performance of our suggested model and produce the best outcomes, the parameters and hyper parameters are adjusted. Depending on the particular needs of our model, several layers were either added or removed from ResNet-50 as an encoder during the fine-tuning process. For deep learning-based image segmentation tasks, the model's fine-tuning time, which included the ResNet50 encoder, was found to be within an acceptable range. Selective layer unfreezing and effective GPU resource utilisation were used to optimise the training process, guaranteeing that the extra time was directly converted into better performance measures.

Table 2: Setup used in Experiment

Parameters	Value
Learning Rate	0.001
Optimizer	Adam
Batch Size	32
Momentum	0.9
Number of Epochs	25
Activation function	ReLu, Softmax
Loss function	Categorical cross-entropy
Image resolution	256 x 256 x 3

Interpretative Analysis

The HRU model has an overall training and validation accuracy for 25 epochs of 94.07% and 94.21%, with training and validation loss values of 0.0447 and 0.0536. Figure 9 shows the accuracy of the HRU model during training and validation. The y-axis shows accuracy percentages, while the x-axis shows the number of epochs. This demonstrates how the training and validation sets are appropriately divided and devoid of over fitting. Figure 10 shows the training and validation losses over epochs for the HRU model. The HRU model optimises an architecture using its loss

function. The loss is computed and interpreted based on the model's performance in the training and validation sets. It is the sum of all mistakes committed for each example in training or validation sets. At the 25th epoch, the validation loss did not drop from 0.0536. The mean IoU value is 0.9199. It demonstrates that the boundaries and patterns of the sick area within the leaf have been accurately represented by the model. Apart from that during the training process, 9058644 trainable parameters are learnt and adjusted, and 23502470 non-trainable parameters are not used in back propagation updates.

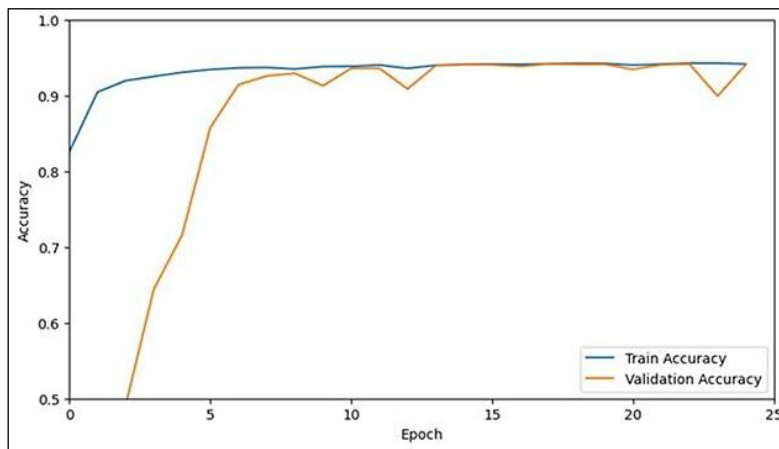


Figure 9: Accuracy versus Epochs

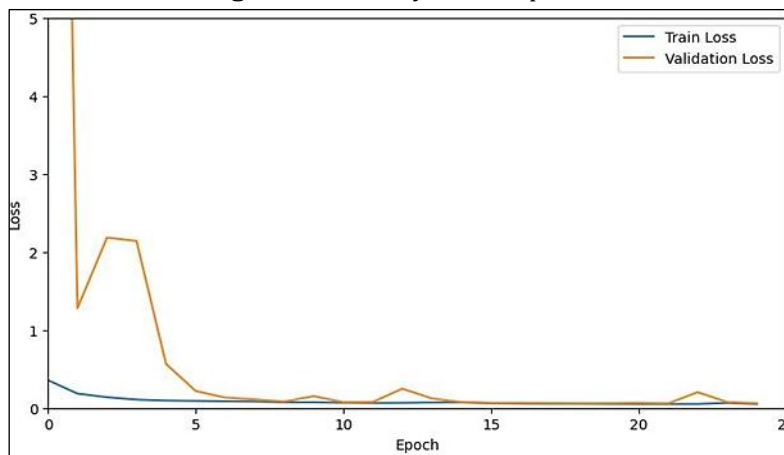


Figure 10: Loss versus Epochs

The suggested HRU model's experimental findings for the semantic segmentation of illnesses found in stone fruit leaves are acquired. The original leaf masks and those predicted by the suggested model are displayed in the results. Figure 11 display the detection outcome of the suggested HRU model's

semantic segmentation for diseased areas on peach bacterial spot. These outcomes demonstrate how well the suggested methodology worked, producing respectable semantic segmentation results.

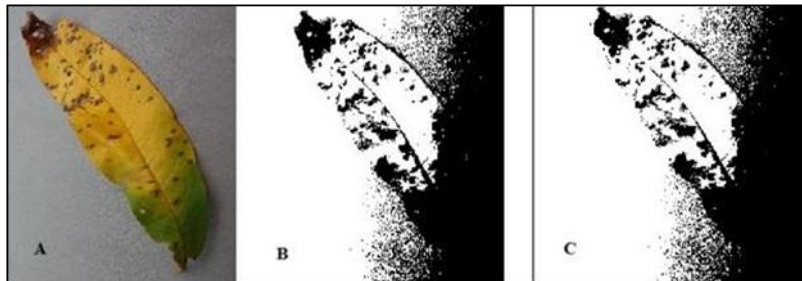


Figure 11: A) Original Leaf Image B) Image Segmentation Mask C) Segmentation Prediction

Additionally, lesions from two or more illnesses may overlap within a leaf; however, in our study, we have only used a single leaf from a single disease. The rarest dataset is for several lesions on a single leaf. Our sophisticated crop disease detection model's effectiveness was carefully evaluated through the use of specific performance criteria. Precision, recall, F1-score, and support were used to measure the model's ability to discriminate between different crop illnesses and healthy states for each categorised category. These measures, which provided both specific insights and a comprehensive picture of the model's performance, were computed for each class separately as well as average values across all classes. Figure 12 displays the class-wise classification report with graphical representation. With an F1-score of 0.98 for Mango Bacterial Canker, the HRU model demonstrated nearly perfect identification with great precision (0.96) and perfect recall (1.00). With maximum precision and recall ratings of 1.00, Mango Healthy showed flawless performance, suggesting that no healthy mango sample was misclassified. The model performed well in classifying Mango Powdery Mildew, with a precision and recall of 0.91 and

0.91, respectively. Notably, an F1-score of 0.95 indicates a balanced performance. Additionally, the model demonstrated exceptional precision (1.00) and recall (0.99) for olive stone fruit for the disease Olive Aculus, resulting in an F1-score of 0.99, indicating the model's strong capacity for condition detection. Olive Healthy earned an F1-score of 0.87 with a lower recall of 0.83 and a precision of 0.92. This decreased recall suggests that correctly classifying every occurrence of a healthy olive may present certain difficulties. However, Olive Peacock has a precision value of 0.95 and an F1-score of 0.95 as a result of a perfect recall of 1.00, indicating exceptional accuracy in identifying this illness. The most common illness for peach stone fruit, Peach Bacterial Spot, had precision of 0.95 and recall of 0.83, which together produced an F1-score of 0.97 for peach stone fruit, indicating accurate but sometimes erratic detection. Additionally, the Peach Healthy model demonstrated strong recall (0.95) and precision (0.91), attaining an F1-score of 0.95, signifying dependable performance. Meanwhile, the Peach Rust model demonstrated exceptional detection with a precision of 0.96 and flawless recall (1.00), albeit with a lower F1-score of 0.91.

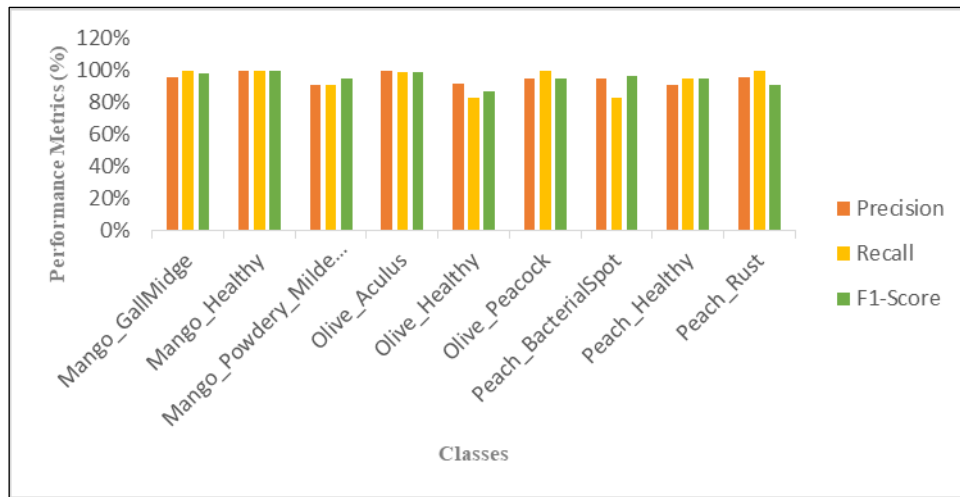


Figure 12: Graphical Class-Wise Report of HRU Model

Performance Comparison

This section will compare the accuracy, recall, and F1-score for individual classes of the HRU model with other models in terms of identifying and

categorising different leaf diseases in stone fruits. A thorough assessment of each model's efficacy was provided by evaluating it for a particular set of stone fruit illnesses.

Table 3: Class-Wise Comparison of HRU Model with other Work Done

Model	Class	Precision	Recall	F1-Score
(11, 31)	Mango_powdery_mildew	91%	89%	90%
	Mango_gall_midge	98.30	96.6	97.4
	Mango_healthy	88%	99%	90%
(32)	Olive_aculus	90.0%	88.0%	85.0%
	Olive_peacock	86.0%	87.0%	86.0%
	Olive_healthy	92.0%	80.0%	84.0%
(33)	Peach_bacterial_spot	99.0%	95.0%	97.0%
	Peach_rust	-	-	-
	Peach_healthy	75.0%	100%	85%
Proposed Model	HRU Mango_powdery_mildew	91.0%	91%	95%
	Mango_gall_midge	96.0%	100%	98%
	Mango_healthy	100%	100%	100%
	Olive_aculus	100%	99%	99%
	Olive_peacock	95%	100%	95%
	Olive_healthy	92%	83%	87%
	Peach_bacterial_spot	95%	83%	97%
	Peach_rust	96%	100%	91%
	Peach_healthy	91%	95%	95%

Mango powdery mildew, Mango gall midge, and Mango healthy are the three main diseases that researchers focused on with mango stone fruit (11). Table 3's values demonstrate good performance in identifying Mango_gall_midge with high recall (96.6%) and precision (98.3%), yielding a superior F1-score of 97.4%. On the other hand, Mango_healthy has a high recall rate (99%), but a very low precision rate (88%), suggesting a higher incidence of false positives for healthy mangoes. Researchers investigated the olive category of

stone fruits in order to treat the Olive healthy, Olive_aculus, and Olive peacock disorders (32). Olive_aculus and Olive peacock exhibit balanced performance, with comparable precision and recall values, resulting in consistent F1-scores of approximately 85-86%. Olive healthy has a high precision (92%), but a low recall (80%), suggesting that the model is more conservative and producing more false negatives than false positives. Researchers investigated peach stone fruit illnesses, specifically peach rust, peach

bacterial spot, and peach healthy (33). Obtaining an F1-score of 97%, the study demonstrates that excels at detecting Peach_bacterial_spot with near-perfect precision (99%) and good recall (95%). Peach healthy, on the other hand, has 100% recall but just 75% precision, indicating a high number of false positives. Peach rust data is unavailable, which makes a thorough analysis difficult. Mango_powdery_mildew, Mango_gall_midge, Mango healthy, Olive_aculus, Olive peacock, Olive healthy, Peach_bacterial_spot, Peach_rust, and Peach healthy are the nine classes that HRU model conducted trials on. The HRU model performs exceptionally well overall in all classes, with Mango healthy receiving especially high marks (perfect scores of 100% in all criteria). Additionally, it does well in other classes, including Olive_aculus (F1-Score 99%), Peach healthy (F1-Score 95%), and Mango_gall_midge (F1-Score 98%). This model's resilience and generalizability are demonstrated by its consistently good metrics over a wider variety of classes. Drawing from the aforementioned discourse, the following comparative study is conducted: Efficiency: While

studies exhibit good recall and precision for certain disorders, they do not provide thorough coverage for other classes (11, 33). The model performs rather well overall across fewer classes, with opportunity for improvement, especially in Olive healthy (32). The HRU model is the most efficient model overall because of its broad class coverage and consistently high-performance measures. Generalisation: The HRU model outperforms the other models in terms of consistency and range of accurate detection, demonstrating strong generalisation across a variety of stone fruits and diseases. Specificity vs. Sensitivity: Researchers demonstrate good specificity for some diseases (such as Mango_gall_midge and Peach_bacterial_spot), but at the expense of decreased sensitivity in other ailments (11, 33). While it falls short in both specificity and sensitivity, another study manages to strike a balance between the two (32). Over a broad spectrum of illnesses, the suggested HRU model yields a high degree of both specificity and sensitivity that is well-balanced.

Table 4: Comparison of HRU Model with other State-of-the-Art Models

Reference	Model	Accuracy	Number of Epochs
(11)	CNN model (Alexnet)	89%	Not mentioned
(32)	CNN model (VGG16 and VGG19)	95.00%	100
(33)	CNN model	95.26%	35
(34)	Queue-and-excitation SSD, deep block SSD model	92.20%	100
(35)	YOLOv5 network model	86.5%	Not mentioned
Proposed model	HRU model	95.00%	25

Table 4 illustrates how the performance and methodology of the different models for crop disease detection are noticeably different when compared. The CNN models utilised in studies achieved accuracy of 89%, 95%, and 95.26% respectively, by using conventional CNN architectures without including picture segmentation techniques (11, 33, 34). These models did not make use of sophisticated feature extraction or attention methods, but they did show how well deep convolutional networks detect crop illnesses. The deep convolutional neural network used a deep block SSD and squeeze-and-excitation SSD methodology, adding attention mechanisms for improved feature extraction (34). While object detection model i.e. YOLOv5 network for object detection and obtained an accuracy of 86.5%, this

model attained an accuracy of 92.20% across 100 epochs, suggesting that attention processes can greatly boost detection skills by emphasising relevant aspects (35). While YOLO's real-time item identification skills are useful for real-world field applications, its accuracy was not as good as models that used deeper networks and segmentation techniques to focus on disease categorisation. The suggested model used a hybrid technique that included a ResNet-50 encoder with U-Net to achieve overall 95% testing accuracy on unseen data in less than 25 epochs. Graphical representation is shown in Figure 13 below. By combining the strong feature extraction skills of ResNet-50 with the reliable segmentation capabilities of U-Net, this combination produced a crop disease detection model that was incredibly

accurate and efficient. In general, models with attention mechanisms, segmentation algorithms, and sophisticated feature extraction approaches performed better in terms of accuracy and training efficiency. In crop disease detection tasks, the HRU

model distinguished itself by attaining high accuracy in fewer epochs, highlighting the significance of combining segmentation approaches and deep feature extraction networks.

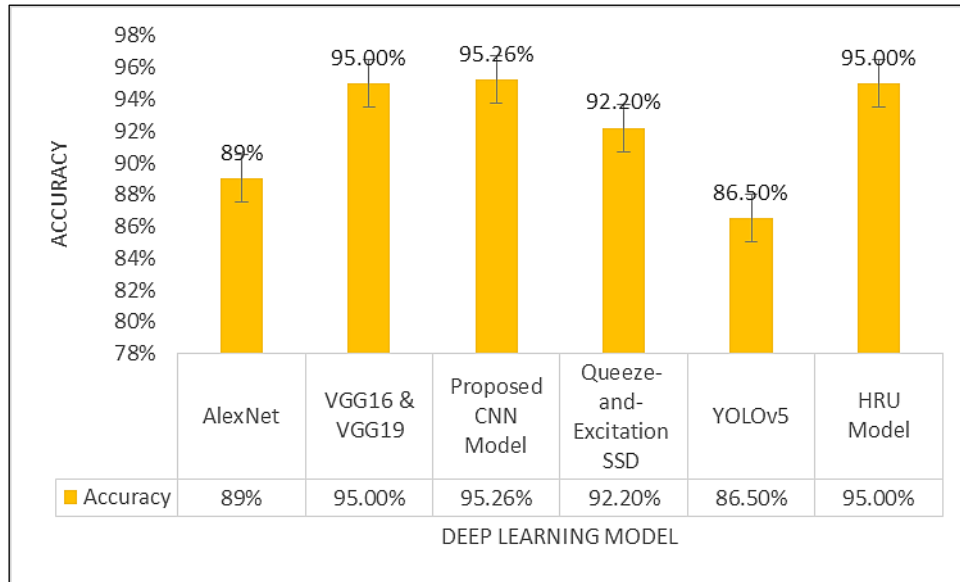


Figure 13: Accuracy Comparison with Other Models

Conclusion

The segmentation and detection of biotic lesion patches of stone fruit leaves is an extremely difficult process because of numerous interconnected factors, including ambient lighting, a complex backdrop, a diversity of symptom symptoms, and more. This study presents a novel HRU model that is built on the ResNet-U-Net framework and uses the ResNet-50 architecture as the U-Net model's structural foundation. The network's weights are updated via the ADAM optimiser. When compared to the most advanced methods now in use for identifying leaf disease in nine different classes of stone fruits, the suggested model produced superior results. The decoder portion of the system concatenates and up-samples the high-level feature maps that the ResNet-50 architecture extracted. The suggested HRU model's produced results demonstrate the architecture's usefulness. After the experiment was analysed, it was discovered that the hybrid Residual U-Net (HRU) model was able to segment the lesion region properly in every environmental state, achieving testing accuracy of 95% with 25 epochs on a hybrid dataset. Even though the suggested HRU model solves the present demand for precise leaf disease segmentation, some issues still exist. This study is still limited by two major

concerns. First, there is need to improve the detection of tiny lesions, which are sometimes challenging to accurately segment. Second, even though a single segmentation approach (UNet+ResNet-50) worked well, more research into hybrid or multi-stage approaches may improve classification results. Furthermore, the ResNet-50 encoder's depth results in a comparatively large computational burden for the model, which could impact its real-time deployment on edge devices. Subsequent research endeavours may investigate lightweight substitutes like Mobile-Net or employ model compression methods like quantisation and pruning. With these enhancements, the model might be more suited for real-time agricultural applications with constrained processing power.

Abbreviations

None.

Acknowledgement

None.

Author Contributions

Sonali Goyal: conceived the study conception and design, Manju Bagga: conceived the study conception and design, wrote the first version of manuscript as well as reviewed and edited the

manuscript. All the authors have read and approved the final manuscript.

Conflict of Interests

The authors declare that they have no competing interests.

Ethics Approval

Not applicable.

Funding

This research did not receive any specific funding.

References

1. Yadav S, Sengar N, Singh A, Singh A, Dutta MK. Identification of disease using deep learning and evaluation of bacteriosis in peach leaf. *Ecological Informatics*. 2021 Mar 1; 61:101247.
2. Bagga M, Goyal S. Image-based detection and classification of plant diseases using deep learning: State-of-the-art review. *Urban Agriculture & Regional Food Systems*. 2024; 9(1):e20053.
3. Wang CL, Lu CY, Chen WZ, Li HW, He J, Wang QJ. Image segmentation of maize stubble row based on genetic algorithm and threshold filtering noise. *Trans Chin Soc Agric Eng*. 2019; 16:198-205.
4. Esgario JG, Krohling RA, Ventura JA. Deep learning for classification and severity estimation of coffee leaf biotic stress. *Computers and Electronics in Agriculture*. 2020; 169:105162.
5. Agarwal M, Gupta SK, Biswas KK. Development of Efficient CNN model for Tomato crop disease identification. *Sustainable Computing: Informatics and Systems*. 2020; 28:100407.
6. Aldakheel EA, Zakariah M, Alabdall AH. Detection and identification of plant leaf diseases using YOLOv4. *Frontiers in Plant Science*. 2024; 15:1355941.
7. Abd Algani YM, Caro OJ, Bravo LM, Kaur C, Al Ansari MS, Bala BK. Leaf disease identification and classification using optimized deep learning. *Measurement: Sensors*. 2023; 25:100643.
8. Jafar A, Bibi N, Naqvi RA, Sadeghi Niaraki A, Jeong D. Revolutionizing agriculture with artificial intelligence: plant disease detection methods, applications, and their limitations. *Frontiers in Plant Science*. 2024; 15:1356260.
9. Boulent J, Foucher S, Theau J, St Charles PL. Convolutional neural networks for the automatic identification of plant diseases. *Frontiers in plant science*. 2019; 10:941.
10. Sharma P, Berwal YP, Ghai W. Performance analysis of deep learning CNN models for disease detection in plants using image segmentation. *Information Processing in Agriculture*. 2020; 7(4):566-74.
11. Rao US, Swathi R, Sanjana V, Arpitha L, Chandrasekhar K, Naik PK. Deep learning precision farming: grapes and mango leaf disease detection by transfer learning. *Global transitions proceedings*. 2021; 2(2):535-544.
12. Bezabh YA, Ayalew AM, Abuhayi BM, Demlie TN, Awoke EA, Mengistu TE. Classification of mango disease using ensemble convolutional neural network. *Smart Agricultural Technology*. 2024; 8: 100476.
13. Ronneberger O, Fischer P, Brox T. U-net: Convolutional networks for biomedical image segmentation. In *Medical image computing and computer-assisted intervention-MICCAI 2015: 18th international conference, Munich, Germany, October 5-9, 2015, proceedings, part III 18 2015* (pp. 234-241). Springer international publishing. https://doi.org/10.1007/978-3-319-24574-4_28
14. He K, Zhang X, Ren S, Sun J. Deep residual learning for image recognition. In *Proceedings of the IEEE conference on computer vision and pattern recognition*. 2016; (pp. 770-778). <https://ieeexplore.ieee.org/document/7780459>
15. Litjens G, Kooi T, Bejnordi BE, Setio AAA, Ciompi F, Ghafoorian M, Sanchez CI. A survey on deep learning in medical image analysis. *Medical image analysis*. 2017; 42:60-88.
16. Sujatha R, Chatterjee JM, Jhanjhi NZ, Brohi SN. Performance of deep learning vs machine learning in plant leaf disease detection. *Microprocessors and Microsystems*. 2021; 80:103615.
17. Agarwal M, Gupta S, Biswas KK. A new Conv2D model with modified ReLU activation function for identification of disease type and severity in cucumber plant. *Sustainable Computing: Informatics and Systems*. 2021; 30:100473.
18. Nair V, Hinton GE. Rectified linear units improve restricted boltzmann machines. In *Proceedings of the 27th international conference on machine learning (ICML-10)*. 2010; (pp. 807-814). <https://www.cs.toronto.edu/~hinton/absps/reluICML.pdf>
19. Alshammari HH, Taloba AI, Shahin OR. Identification of olive leaf disease through optimized deep learning approach. *Alexandria Engineering Journal*. 2023; 72:213-224.
20. Bocca P, Orellana A, Soria C, Carelli R. On field disease detection in olive tree with vision systems. *Array*. 2023; 18:100286.
21. Chen SY, Lin C, Li GJ, Hsu YC, Liu KH. Hybrid deep learning models with sparse enhancement technique for detection of newly grown tree leaves. *Sensors*. 2021; 21(6):2077.
22. Jain A, Sarsaiya S, Wu Q, Lu Y, Shi J. A review of plant leaf fungal diseases and its environment speciation. *Bioengineered*. 2019; 10(1):409-424.
23. Rashid J, Khan I, Ali G, Almotiri SH, AlGhamdi MA, Masood K. Multi-level deep learning model for potato leaf disease recognition. *Electronics*. 2021; 10(17):2064.
24. Pham TN, Van Tran L, Dao SV. Early disease classification of mango leaves using feed-forward neural network and hybrid metaheuristic feature selection. *IEEE access*. 2020 Oct 19; 8:189960-73.
25. Mana SC, Sasipraba T. An intelligent deep learning enabled marine fish species detection and classification model. *International Journal on Artificial Intelligence Tools*. 2022; 31(01):2250017.
26. Huang S, Zhou G, He M, Chen A, Zhang W, Hu Y. Detection of peach disease image based on asymptotic non-local means and PCNN-IPELM. *IEEE Access*. 2020; 8:136421-136433.
27. Gohane R, Adatrao S, Mittal M. Comparison of various centroiding algorithms to determine the centroids of

- circular marks in images. In 2016 International Conference on Computing, Analytics and Security Trends (CAST) (pp. 162-166). IEEE.
<https://ieeexplore.ieee.org/abstract/document/7914959>
28. Weng W, Zhu X. INet: convolutional networks for biomedical image segmentation. *IEEE Access*. 2021; 9:16591-16603.
 29. Powers DM. Evaluation: from precision, recall and F-measure to ROC, informedness, markedness and correlation. arXiv preprint arXiv:2010.16061. 2020 Oct 11. <https://arxiv.org/abs/2010.16061>
 30. Garcia-Garcia A, Orts-Escolano S, Oprea S, Villena-Martinez V, Garcia-Rodriguez J. A review on deep learning techniques applied to semantic segmentation. arXiv preprint arXiv: 2017.1704.06857. <https://arxiv.org/pdf/1704.06857>
 31. Rajbongshi A, Khan T, Pramanik MMRA, Tanvir SM, Siddiquee NRC. Recognition of mango leaf disease using convolutional neural network models: a transfer learning approach. *Indonesian Journal of Electrical Engineering and Computer Science*. 2021; 23(3):1681-1688.
 32. Uguz S, Uysal N. Classification of olive leaf diseases using deep convolutional neural networks. *Neural computing and applications*. 2021; 33(9), 4133-4149.
 33. Tusher AN, Islam MT, Sammy MSR, Hasna SA, Chakraborty NR. Automatic Recognition of Plant Leaf Diseases Using Deep Learning (Multilayer CNN) and Image Processing. In *International Conference on Image Processing and Capsule Networks*. 2022. (pp. 130-142). Cham: Springer International Publishing. https://link.springer.com/chapter/10.1007/978-3-031-12413-6_11
 34. Wang J, Yu L, Yang J, Dong H. DBA_SSD: A novel end-to-end object detection algorithm applied to plant disease detection. *Information*. 2021; 12(11):474.
 35. Chen Z, Wu R, Lin Y, Li C, Chen S, Yuan Z, Zou X. Plant disease recognition model based on improved YOLOv5. *Agronomy*. 2022; 12(2):365.